Title	Average velocity of solitary coarse grain in flows over smooth and rough beds
Author(s)	Cheng, Nian-Sheng; Emadzadeh, Adel
Citation	Cheng, N.-S., & Emadzadeh, A. (2014). Average velocity of solitary coarse grain in flows over smooth and rough beds. Journal of hydraulic engineering, 140(6).
Date	2014
URL	http://hdl.handle.net/10220/25370
Rights	© 2014 American Society of Civil Engineers. This is the author created version of a work that has been peer reviewed and accepted for publication by Journal of Hydraulic Engineering, American Society of Civil Engineers. It incorporates referee’s comments but changes resulting from the publishing process, such as copyediting, structural formatting, may not be reflected in this document. The published version is available at: [Article DOI: http://dx.doi.org/10.1061/(ASCE)HY.1943-7900.0000875].

Average velocity of solitary coarse grain in flows over smooth and rough beds

Nian-Sheng Cheng

School of Civil and Environmental Engineering,

Nanyang Technological University, Nanyang Avenue, Singapore.

Email: cnscheng@ntu.edu.sg

Adel Emadzadeh

School of Civil and Environmental Engineering,

Nanyang Technological University, Nanyang Avenue, Singapore.

Email: ADEL0006@e.ntu.edu.sg

Average velocity of solitary coarse grain in flows over smooth and rough beds

Nian-Sheng Cheng

School of Civil and Environmental Engineering,

Nanyang Technological University, Nanyang Avenue, Singapore.

Email: cnscheng@ntu.edu.sg

Adel Emadzadeh

School of Civil and Environmental Engineering,

Nanyang Technological University, Nanyang Avenue, Singapore.

Email: ADEL0006@e.ntu.edu.sg

Abstract. A formula is derived for the prediction of the average velocity of a solitary coarse grain moving over a rigid flat channel bed. To verify the theoretical consideration, data collected in the present study and reported in the literature (811 sets in total) are analyzed for typical bed roughness configurations. The results show significant improvements in the prediction of solitary grain velocity for both smooth and rough bed conditions, in comparison with other formulas available in the literature. From the proposed formula, it follows that for rough bed conditions, the dimensionless grain velocity depends on the Shields number and also the ratio of bed roughness height to the grain diameter. The present study is limited to motion of solitary grains, but the result obtained implies that bedload transport rate could be

also affected by the equivalent bed roughness height even under mobile bed conditions and such effects may become pronounced for non-uniform sediments.

Keywords: grain velocity; bedload; smooth bed; rough bed; bed roughness; bed shear stress

Introduction

Bedload transport rate can be estimated as a product of average grain velocity, bedload thickness and sediment concentration (Bagnold, 1973, Bridge and Dominic, 1984). However, how to quantify each individual factor, theoretically or even experimentally, still remains challenging at present because of complex near-bed flow phenomena and fluid-grain and grain-grain interactions. To simplify relevant physical phenomena, laboratory observations of sediment motion near the bed could focus only on a solitary bedload grain. Such simplifications do not result in a general formula for the computation of bedload transport rate, but they provide important insights into dynamics of the near-bed sediment motion (Francis, 1973).

In this paper, all information presented will be largely associated with a solitary grain moving near the bed. The grain velocity is defined as the average velocity of the grain moving continuously over a channel reach, of which the length is a few orders greater than the grain diameter. First, previous studies related to the calculation of bedload grain velocity are reviewed. Then, a new formula is derived by considering forces exerting on a moving grain in the context of spatial average. To substantiate the theoretical consideration, experimental data from the literature and collected in the present study are analyzed for typical bed configurations. The results show that the new formula represents well observed bedload grain velocities in flows over smooth and rough channel beds of different roughness.

Previous Formulas

Several empirical and analytical formulas for predicting bedload grain velocity have been reported in the literature, as summarized in Table 1. One of the early efforts is due to Einstein (1950), who proposed that the average bedload velocity is proportional to the shear velocity with respect to the grain. Bagnold (1973) assumed that the difference between the local fluid velocity at the representative height of a saltating grain and the grain velocity can be approximated to be the settling velocity. Fernandez Luque and van Beek (1976), Abbott and Francis (1977) and Bridge and Dominic (1984) developed their formulas individually based on the fact that the observed grain velocity appears to be linearly related to the bed shear velocity. Some regression analyses have been done by van Rijn (1984), Wu et al. (2006) [also see Wu (2008)], and Julien and Bounvilay (2013), and their formulas implicitly include viscous effects of fluid on the motion of bedload grain near the bed.

For comparison purposes, the previous formulas in Table 1 are presented in terms of the dimensionless grain velocity χ defined as

$$\chi = \frac{u_s}{\sqrt{\Delta g D}} \tag{1}$$

and the dimensionless bed shear stress or Shields number θ,

$$\theta = \frac{u_*^2}{\Delta g D} \tag{2}$$

In Eqs. (1) and (2), u_s is the grain velocity, u_* is the shear velocity, Δ [= $(\rho_s - \rho)/\rho$] is the effective specific density, ρ is the fluid density, ρ_s is the grain density, g is the gravitational acceleration and D is the grain diameter. The other dimensionless parameters used include the dimensionless grain diameter D_*,

$$D_* = \left(\frac{\Delta g}{\nu^2}\right)^{1/3} D \tag{3}$$

where ν is the kinematic viscosity of fluid, and transport stage parameter T_*,

$$T_* = \frac{\theta - \theta_c}{\theta_c} \tag{4}$$

where θ_c is the critical Shields number for the incipient sediment motion.

By comparing the previous formulas, two observations can be made. First, the critical bed shear stress for the incipient sediment motion has been used in almost all the previous studies. As a result, the formulas would fail to predict the grain velocity if the bed shear stress is less than the critical value for initial sediment motion. The application of the concept of the critical bed shear stress in the formulas is based on the argument that a bedload grain does not move if the bed shear stress is less than its critical value. However, this argument may not hold generally. After reviewing historical data for the incipient sediment motion, Lavelle and Mofjeld (1987) concluded that the critical shear stress should not be included as an essential parameter in the investigation of bedload transport rates. Paintal (1971) observed that there is no shear stress below which no single grain moves. Laursen (1999) noticed that the same sediment particle has as many values of the critical shear stress as there are sediment transport formulas. Therefore, it is not necessary to involve the critical bed shear stress in the formulation of the bedload grain velocity as well as the bedload transport rate (Cheng, 2002).

The second observation is that only Julien and Bounvilay (2013) included the effect of the bed roughness on the bedload grain velocity, and the other formulas were basically developed for the condition of the moving grain being the same as the sediment bed material. However, it should be noted that the formula by Julien and Bounvilay (2013) is not applicable for smooth beds with the bed roughness size approaching zero.

In this study, both smooth and rough bed configurations are considered in performing laboratory experiments and data analysis, and also in developing a new formula for calculating solitary grain velocity. In particular, the critical bed shear stress or velocity is not directly involved in the calibration of the formula proposed. With 811 sets of experimental data compiled from 11 sources, the evaluation of the bedload grain velocity is discussed in detail for different bed configurations.

Theoretical Consideration

First, the grain velocity under consideration is taken to be the average velocity of the grain that moves over a channel reach. Being different from the local grain velocity, the average grain velocity is one-dimensional and has no vertical and transverse components. Therefore, it can be described using a one-dimensional mathematical model. Here we consider a sediment grain of diameter D moving along the channel bed at average velocity u_s, which is usually subject to the drag force F_D, the lift force F_L, the bed resistance F_R, and the submerged weight W (see Fig. 1). The drag force is expressed as

$$F_D = C_D \frac{\pi D^2}{4} \frac{\rho (u_s - u_b)^2}{2} \tag{5}$$

where C_D is the drag coefficient and u_b is the unobstructed, near-bed flow velocity that is evaluated at a representative height of the moving grain. The submerged weight of the grain is

$$W = \Delta\rho g \frac{\pi D^3}{6} \tag{6}$$

The resistance F_R is due to the grain-bed interaction and can be expressed as

$$F_R = W \cos\beta \tan\alpha \tag{7}$$

where β is the slope angle, $\tan\alpha$ is the friction coefficient and α is the friction angle. If $u_b > u_s$, F_D is in the direction towards downstream. Therefore, the following momentum equation applies in the streamwise direction,

$$F_D + W \sin\beta = F_R \tag{8}$$

It is noted that the lift force is ignored here. Locally, the lift force is important in the investigation of local movements, e.g. a particular grain trajectory. However, in the one-dimensional model, it is assumed that the grain moves only in the streamwise direction. As a result, all forces are taken to be space-averaged in the channel reach under consideration. This implies that the bed-normal lift force can be excluded for consideration.

Substituting Eqs. (5) to (7) into Eq. (8),

$$\chi = \frac{u_b}{\sqrt{\Delta g D}} - \sqrt{\frac{4}{3}\frac{\cos\beta\tan\alpha - \sin\beta}{C_D}} \tag{9}$$

Eq. (9) applies for the condition of $u_b > u_s$ and the second term on the right-hand-side implies that the slope angle is smaller than the friction angle, i.e. $\beta < \alpha$. By taking $u_b = c_1 u_*$, where c_1 is a coefficient and assuming that β is much smaller than α, Eq.(9) can be rewritten as

$$\chi = c_1\sqrt{\theta} - \sqrt{\frac{4}{3}\frac{\tan\alpha}{C_D}} \tag{10}$$

It is noted that equations similar to Eq. (9) or (10) have been also proposed previously by van Rijn (1984), Bridge and Dominic (1984) and Fredsoe and Deigaard (1992). Both Eqs. (9) and (10) are simple but not practically useful. This is because difficulties are often encountered in the evaluation of the three coefficients, c_1, $\tan\alpha$ and C_D due to complex dynamics of near-bed flow and grain-bed interaction. In the following, we will first discuss to what extent the coefficients can be fixed, and then simplify Eq. (10) for some cases.

Estimate of c_1

By noting that c_1 is the ratio of u_b to u_*, its value depends on the choice of a representative distance y_b (from the center of the moving grain to the channel bed), at which u_b is determined. For a flat bed, whether smooth or rough, c_1 can be estimated according to the near-bed velocity profile (Cheng, 2008),

$$c_1 = \left\{ (y_b^+)^{-3} + \left[2.5\ln\left(1 + \frac{9y_b^+}{1 + 0.3k_s^+(1 - e^{-0.04k_s^+})} \right) \right]^{-3} \right\}^{-1/3} \tag{11}$$

where $y_b^+ = u_* y_b/\nu$, $k_s^+ = u_* k_s/\nu$ and k_s is the equivalent roughness height of the channel bed. Eq. (11) describes the linear velocity distribution in the viscous sublayer, the logarithmic profile in the inertial flow zone, and also the transition in between. From Eq. (11), it follows that the calculation of c_1 is subject to the representative height y_b, which varies in the order of D, and equivalent roughness height k_s, which depends on the bed material and its mobility.

Variation of α with bed roughness

For natural sediments, the friction angle is markedly affected by particle shape and size distribution. Wiberg and Smith (1987) suggested that the friction angle varies between 50^o and 60^o for well-sorted natural sands. Johnston et al. (1998) conducted in situ determination of friction angles of fluvial gravels, showing that the average friction angle varied from 49.1^o to 61.9^o for median sediment grains. Similar results have been also reported by Buffington et al. (1992). Significant changes in the friction angle occur when the grain in motion is different from the bed sediment. A few theoretical and empirical formulas have been proposed in previous studies to relate α to the ratio of k_s to D. For example, by considering a sphere of diameter D moving from its position of rest in a bed of spheres of diameter k_s, Miller and Byrne (1966) showed that the friction coefficient can be theoretically related to D/k_s,

$$\tan\alpha = \frac{0.866}{\sqrt{(D/k_s)^2 + 2(D/k_s) - 0.333}} \quad (12)$$

Eq. (12) can be further approximated in terms of the power-law. For example, for $k_s/D < 1$, Eq. (12) is close to the following function,

$$\tan\alpha = 0.54\left(\frac{k_s}{D}\right)^{0.8} \quad (13)$$

or

$$\alpha = 28\left(\frac{k_s}{D}\right)^{0.75} \quad (14)$$

Experimental data show that Eqs. (12) and (13) generally underestimate the friction angle but predict the trend of its variation with k_s/D reasonably (Miller and Byrne, 1966). The power-law function, with varying coefficient and exponent, has been found very useful in representing field measurements of the friction angle (Buffington, Dietrich and Kirchner, 1992). In the subsequent analysis, the power-law relation between $\tan\alpha$ and k_s/D, with undefined coefficient and exponent, will be used to simplify Eq. (10).

Estimate of C_D

For the motion of a grain without any boundary effect, the drag coefficient C_D can be calculated using empirical formulas (Cheng, 1997, Cheng, 2009). In the presence of a boundary, C_D may increase with the grain proximity to the boundary, which is not well understood at present. With the information of boundary effects on settling velocity summarized by Chien and Wan (1999), the drag coefficient in the presence of the boundary could be formulated as $[1+(9/32)(D/s)]^2C_D$, where s is the distance from the center of the moving grain to the boundary. With this simple function, it can be estimated that C_D increases by 60% if s/D = 1 and by 20% if s/D = 3. In comparison, only a small increase in

C_D was observed in laboratory measurements. For example, Nakagawa and Tsujimoto (1981) reported that for a sphere placed on a rough bed composed of spheres of the same kind, the value of C_D remained unchanged or increased slightly, in comparison with that for a free falling sphere. Similar findings were also presented by Schmeeckle et al. (2007).

From the foregoing discussions, it follows that there are no complete approaches available at present for determining c_1, tanα and C_D. This renders that Eq. (10), though simple, is inapplicable for predicting the bedload grain velocity directly. However, on the other hand, Eq. (10) can be simplified for some cases. For example, for a smooth channel bed, for which k_s is much smaller than D and tanα approaches zero, Eq. (10) reduces to

$$\chi = c_1\sqrt{\theta} \tag{15}$$

Another simplification can be made possible for the case of coarse bedload grains, e.g. natural gravels of D ≥ 2 mm, for which the viscous effect on the drag coefficient can be ignored and then C_D can be approximated as a constant (Cheng, 1997). If tanα is expressed as a power-law function of k_s/D, similar to Eq. (13), Eq. (10) is rewritten as

$$\chi = c_1\sqrt{\theta} - c_2\left(\frac{k_s}{D}\right)^m \tag{16}$$

where c_2 is a coefficient and m is an exponent, both being positive. It is noted that Eq. (16) reduces to Eq. (15) when k_s is much smaller than D. As shown in the following section, most of the experimental data compiled in the present study were collected either under smooth-bed conditions or with coarse grains, and thus they can be used to evaluate c_1, c_2 and m in Eq. (16).

Data Analysis

Experimental data used for analysis consist of two parts. The first part, comprising 96 sets, was generated from the experiments conducted in the present study, as described subsequently. The second part, comprising 715 sets, was reproduced from the previous studies (Abbott and Francis, 1977, Fernandez Luque and van Beek, 1976, Francis, 1973, Hu and Hui, 1996, Julien and Bounvilay, 2013, Lee, et al., 2000, Lee and Hsu, 1994, Niño and García, 1998, Niño, et al., 1994, Parsons, 1972). A summary of the data is shown in Table 2.

In the previous studies, most of the experiments were conducted under the condition of the moving grain taken the same as uniform sediment bed materials (Abbott and Francis, 1977, Francis, 1973, Lee, Chen, You and Lin, 2000, Lee and Hsu, 1994, Niño, García and Ayala, 1994). To facilitate experimental observations, the sediment bed is often prepared by gluing a layer of sediment grains onto the channel bottom, which results in $k_s \approx D$. In comparison, the measurement of the grain velocity under the mobile bed condition is more complicated, and limited efforts have been made by Fernandez Luque and van Beek (1976) and Niño et al. (1994). Different from the others, Julien and Bounvilay (2013) and Bounvilay (2003) investigated effects of the bed roughness height on the grain velocity. They employed a series of moving grains of different sizes when the bed condition remained unchanged, which yielded the relative roughness height k_s/D varying from 0 to 1.0.

All the data can be categorized into four different cases according to the bed conditions (Fig. 2). The first case is related to the experiments conducted under the smooth bed condition, of which the bed roughness height k_s is much smaller than the grain diameter D, i.e. $k_s << D$. The second case involves the investigations with the moving grain and bed material of the same size, i.e. $k_s \approx D$. The third case is limited to the case of $k_s < D$. In the first three cases, the bed, whether smooth or rough, is rigid. The last case concerns the experiments with mobile beds for which $k_s > D$.

In the following, individual data analysis is performed for each case to check applicability of the foregoing theoretical consideration.

Case 1: Smooth bed (k_s << D)

The first case concerns a smooth channel bed, of which the bed roughness height is much smaller than the grain diameter and thus the bed resistance is negligible. Four series of data were selected under this condition.

The first series is due to Parsons (1972) who performed experiments with glass beads and sand grains in laminar flows. To avoid any significant bed friction, only the data with glass beads are used here. It should be mentioned that this is the only data series related to laminar flows that is used in the present study. For laminar flows, the velocity profile near the bed is linear and Eq. (11) reduces to

$$c_1 = \frac{u_* y_b}{\nu} \tag{17}$$

Furthermore, by noting that y_b is proportional to D, Eq. (10) can be rewritten as

$$\chi = c_3 \,\mathrm{Re}_* \sqrt{\theta} - \sqrt{\frac{4}{3}\frac{\tan\alpha}{C_D}} \tag{18}$$

where $\mathrm{Re}_* = u_* D/\nu$ and c_3 is a constant. In Fig. 3, χ is plotted against $\mathrm{Re}_*\sqrt{\theta}$ with the data reported by Parsons (1972) for six different sizes of glass beads (D = 0.25-0.85 mm). It shows that the relationship between χ and $\mathrm{Re}_*\sqrt{\theta}$ is almost linear, which is consistent with Eq. (18). The results also imply that c_3 = 0.27 (and thus y_b = 0.27D) and the bed resistance, represented by the last term on the RHS of Eq. (18), is relatively small.

Next, smooth-bed experiments performed under turbulent flow conditions are examined. For turbulent flows, the ratio of u_b/u_* varies with y_b and k_s [see Eq. (11)]. It can be assumed that y_b is proportional to D and an empirical k_s-value can be assigned to a particular smooth bed. Computations using Eq. (11) show that u_b/u_* increases with increasing Re_*, but varying in a limited range for large Re_*. For example, if taking y_b = 0.27D, as suggested by the laminar flow result, and k_s = (1%-10%)D, u_b/u_* would vary from 11 to 18 for $Re_* > 60$. However, it is not clear how to determine y_b generally for turbulent flows (Bagnold, 1973).

Three series of data for turbulent flows over a smooth bed are employed for analysis, which were generated from the experiments by Hu and Hui (1996) and Julien and Bounvilay (2013) and also by the present study. In Julien and Bounvilay's (2013) experiments (also see Bounvilay (2003)), tested grains comprised glass beads, steel balls and natural sands, but only the data for the glass beads are used here. This selection was made for two reasons. First, the experiments by Julien and Bounvilay's (2013) were conducted under relatively low bed shear stress conditions (θ = 0.000076-0.016), at which the grain velocity could be sensitive to channel bed resistance. Second, in comparison to glass beads, both natural sands and steel balls may induce significant bed resistance because of their angular shape or high density. In comparison, Hu and Hui (1996) carried out their observations with much higher bed shear stresses (θ = 0.15-1.41), for which the effect of the bed resistance on the grain velocity could be considered insignificant in spite of some non-spherical grains tested.

To obtain additional data in the range of the intermediate Shields number (say, θ = 0.01-0.1), similar smooth-bed experiments were also carried out in the present study in an open channel. The channel was 100 mm in width, 150 mm in height and 3000 mm in length, with both the channel wall and bed made of glass. Water was circulated using a centrifugal pump, providing a discharge in the range of 0-1.3 l/s, and the flow rate was measured with an electromagnetic flow meter. Water temperature was measured with a mercury thermometer of an accuracy of 0.1^{o}C and the kinematic viscosity was calculated using $\nu = \left[60/(T+40)\right]^{1.45} 10^{-6}$ (Cheng, et al., 2011), where T is in degree Celsius and ν in m^2/s. Three kinds of spheres with ρ_s/ρ varying from 1.14 to 2.60 were used, which all measured 11 mm in diameter. The flow depth was measured along the channel with a 0.25m interval by applying a pressure transducer through the sidewall. All the experiments were conducted under uniform flow conditions. To achieve a uniform flow, a channel slope was selected first after certain trial tests. Then the flow rate and tailgate were adjusted. This was a trial-and-error process and the slope, tailgate and flow rate could be adjusted several times for a particular test. The flow was assumed fully developed at the test section. This is because the flow depth was usually small. When h varied from 0.0125 m to 0.022 m (see the data included in Table 3), the distance from the beginning of the channel to the test section was equal to (45-80)h (= 1 m). This agrees with the study by Ranga Raju et al (2000), who found that the developing length (required for 99% development of free stream velocity) varied from 40h to 120h for a range of aspect ratios and relative roughness heights.

For each test, a grain was first released near the bed at the beginning of the channel. To obtain the average grain velocity, the time duration was recorded for a grain to complete its journey over a 1.5m channel reach, which started from a section 1m downstream from the flume entrance. Each test was repeated 20 times under the same flow condition. The data collected in the present study are provided in Table 3.

It should be mentioned that sidewall effects were not investigated in this study. During the experiment, grains moving close to sidewalls were not used for measurements, and the relevant tests were repeated. It was observed that typically grains moved almost along the centerline of the channel, even under rough bed conditions. On the other hand, it is also noted that the grain was considered large in comparison with the flow depth. This may cause the experimental results different from those obtained under high submergence conditions. A further discussion in this respect will be provided subsequently.

The three series of data for turbulent flows over smooth beds are plotted in Fig. 4. It shows that the dimensionless grain velocity χ can be linearly related to the square root of the Shields number θ. By ignoring the bed-resistance, the linear relationship can be described with Eq. (15) by taking c_1 = 13.1 with a variation of about ±30%, or in the range of 9.1 to 17.0. This range of c_1 is close to that estimated with Eq. (11) for large Re_*. In processing the data, the shear velocity is taken as $(ghS)^{0.5}$, where h is the flow depth and S is the channel slope, by noting the large aspect ratios applied in all the three experiments.

Case 2: Rigid sediment bed ($k_s \approx D$)

In the second case, the size of the fixed bed roughness element is the same as that of the moving grain tested. Here a further differentiation is made between spherical and non-spherical grains. For spherical tested grain and bed material, 44 sets of data were collected in the present study (see Table 3). The experimental setup was the same as that for the smooth-bed tests but with a sediment bed, which was prepared with a layer of spheres (k_s = 11 mm) placed with the densest arrangement over the entire flume bottom. Fig. 5 shows that for spherical grains, the measured grain velocity can be well represented using Eq. (16) with c_1 = 11.2 and c_2 = 1.0.

For non-spherical tested grain and bed material, in total 125 sets of data reported previously by Francis (1973), Abbott and Francis (1977), Lee and Hsu (1994), Niño and García (1998) and Lee et al. (2000) are used for analysis. Francis (1973) conducted six series of experiments using both natural and artificial grains of different shape and density. All the data are provided in Francis'(1973) paper but without information about the grain densities, which make inconvenient any further analysis of his measurements. However, for series K in his data, it is possible to estimate the grain densities from the measured settling velocity. This is explained as follows. The grains used in series K were cast in the shape of water-worn gravels, having the same size (D = 7.5 mm) but different densities. By noting that the Reynolds number based on the settling velocity varied from 465 to 2798 for this series, it is reasonable to take the drag coefficient to be 1.0 (Cheng, 1997) and then the densities can be estimated from the measured settling velocity. Therefore, the data of series K were used for the present analysis. As shown later, the dimensionless grain velocity so obtained appears to have similar variations to those reported in Abbott and Francis (1977), who continued the effort by Francis (1973). In addition, by considering availability of the necessary information about flow and grain properties, the data of set 3 (with D = 8.82 mm, ρ_s/ρ = 1.2-2.6) reported by Abbott and Francis (1977) were also reproduced from their figure for the present study.

All the experimental data for non-spherical grains with $k_s \approx D$ can be fitted to Eq. (16) with c_1 = 12.5 and c_2 = 1.5, as shown in Fig. 6. It is noted that this c_1-value is close to the average value (c_1 =13.1) obtained for turbulent flows in case 1. In comparison to c_1 (= 12.5) for non-spherical grains, the value of c_1 (= 11.2) for spherical grains appears 10% smaller. This difference is largely caused by the grain shape, but it may be also associated with the small flow depth used in the present experiments with spherical grains. When the flow depth varies in the same order of the grain diameter, the channel resistance can increase significantly (Bathurst, et al., 1981, Ferguson, 2007). This implies that the grain velocity may reduce with a decrease in the ratio of the flow depth to grain diameter.

Case 3: Rigid sediment bed (k_s < D)

In the third case, the bed roughness height is smaller than the diameter of the tested grain. This case has been systematically studied by Julien and Bounvilay (2013) by varying k_s/D between 0 and 1. Some of their data series for natural sediment grains are plotted in Fig. 7, showing variations of χ with θ at different k_s/D-values. Also superimposed in Fig. 7 are two straight lines, one with c_1 = 13.1 for the case of $k_s/D \approx 0$ and the other with c_1 = 12.5 and c_2 = 1.5 for $k_s/D \approx 1$. It shows that the gradient of each line is almost close to each other but the intercept at the vertical axis varies with k_s/D. This implies that c_1 in Eq. (16) can be approximated to be a constant, e.g, $c_1 \approx 13.0$. Then, the values of c_2 and m can be optimized based on the results shown in Fig. 7, which yields $c_2 = 1.5$ and $m = 0.6$. It should be mentioned that the values of the three constants were obtained from the data related to naturally worn sediments or grains of similar shape, and further adjustments could be made for spheres or other shapes of grains once relevant data are available.

Case 4: Mobile sediment bed ($k_s > D$)

This case appears to be more complicated than the first three cases because bedload grains and bed materials become interchangeable. In this case, k_s is usually greater than D but cannot be measured directly. Recking et al. (2008) shows that for flows over flat sediment beds, k_s increases from 2.1D without bedload to 5.3D with intense bedload transport. It may further increase significantly in the presence of bedforms such as ripples and dunes (Chien and Wan, 1999, van Rijn, 1982). Therefore, when fitting Eq. (16) to the data collected under mobile bed conditions, it is expected that the relationship of χ-θ will deviate from that for the condition of $k_s \approx D$.

Due to difficulties encountered in observations under mobile bed conditions, only limited data have been reported in the literature. Fernandez Luque and van Beek (1976) conducted their mobile-bed experiments in a closed conduit with both horizontal and inclined channel beds. To avoid slope effects on the grain velocity, only the data collected under the horizontal bed condition are analyzed here. Niño et al.'s (1994) mobile-bed experiments involved two different natural sediments with mean diameters of 15 and 31 mm. When fitting Fernandez Luque and van Beek's (1976) data [also see Fernandez Luque (1974)] to Eq. (16), we took $c_1 = 13$ as in case 3, and then found $c_2(k_s/D)^m = 2$ (Fig. 8). Similarly, with Niño et al.'s (1994) data, it can be found that $c_2(k_s/D)^m = 3.3$. If taking $c_2 = 1.5$ and $m = 0.6$, it can be shown that k_s/D varies from 1.6 for Fernandez Luque and van Beek's (1976) data to 3.7 for Niño et al.'s

(1994) data. Such variations in k_s/D are consistent with the observation by Recking et al. (2008).

Comparisons with Previous Formulas

In this section, all the previous formulas with known coefficients are used to predict the average velocity of solitary bedload grain, and then the predictions are compared with the measurements (for turbulent flows only) as summarized in Table 2. The critical Shields number was calculated using Whitehouse et al.'s (2000) formula that represents the Shields diagram.

Fig. 9 shows the comparisons for the case of $k_s \approx D$. The predictions are assessed with the average of error defined as |prediction – measurement|/measurement (%), and the errors are summarized in Table 4. It can be seen that the under-predictions are due to the formulas by Fernandez Luque and van Beek (1976), Fredsoe and Deigaard (1992), Lee and Hsu (1994), Lee et al. (2000) and Wu (2008), the over-predictions are associated with the formulas by van Rijn (1984) and Julien and Bounvilay (2013), and the most acceptable predictions are given by the formula by Hu and Hui (1996) and the present study [i.e. Eq. (16) with $c_1 = 13.0$, $c_2 = 1.5$ and $m = 0.6$]. It is also noted that Eq. (16) differs from the previous formulas except for the one by Julien and Bounvilay (2013) in that the previous formulas may fail to predict the grain velocity at low bed shear stresses because of the use of the critical bed shear stress.

Among the previous studies, the effect of bed roughness was considered only by Julien and Bounvilay (2013), their formula is further used to calculate the bedload grain velocity for rough beds of $k_s \leq D$. As shown in Fig. 10(a), the predictions by Julien and Bounvilay's formula agree very well with their own data for $k_s < D$, but showing large deviations for the other data with $k_s \approx D$, which results in an average error of 45.7%. In comparison, Eq. (16)

yields consistent predictions, as shown in Fig. 10(b), of which the average error is 15.7%. This improvement is significant, but not surprising because the three constants were calibrated with the same database.

Next, Eq. (16) is applied to predict the bedload grain velocity for all the data as summarized in Table 2, in spite of possible effects of the grain shape. The comparison (for turbulent flows) is presented in Fig. 11, and the average of the prediction errors is 18.2%. It should be noted that none of the previous formulas can be applied for both smooth and rough bed conditions, and the formula by Julien and Bounvilay (2013), though involving the bed roughness height, cannot be applied to smooth beds. The good agreement shown in Fig. 11 implies that the proposed formula, Eq. (16), is generally applicable for the prediction of the bedload grain velocity under rigid (both smooth and rough) channel bed conditions. The three constants could be further adjusted to take into account the effect of the grain shape.

Conclusions

By reviewing the previous formulas developed for predicting average velocity of solitary bedload grain, two observations are made. First, almost all the previous formulas are subject to the evaluation of the critical condition for incipient sediment motion, and thus may fail to predict the grain velocity at bed shear stresses lower than the critical values. Second, there is no formula that is applicable for both smooth and rough bed conditions. To avoid the shortcomings, a new formula is then developed for the calculation of the bedload grain velocity in the context of spatial average.

The new formula shows that the normalized grain velocity varies with the dimensionless bed shear stress or the Shields number and also the ratio of bed roughness height to the grain diameter. This result applies for motion of solitary grains over rough beds, but it may suggest that bedload transport rate not only depends on the Shields number but also the equivalent bed roughness height even under mobile bed conditions and such dependence may become pronounced for non-uniform sediments.

To calibrate the proposed formula, the experimental data from the present study and those reported in the literature are compiled and analyzed under different flow conditions, including laminar flows over a smooth bed, turbulent flows over a smooth bed, turbulent flows over a rigid rough bed with varying roughness heights, and turbulent flow over a mobile bed. In comparison with seven previous formulas, the new formula, Eq. (16), performs the best in the prediction of the bedload grain velocity for both smooth and rough configurations. In addition, Eq. (16) could be also applied for the mobile bed condition provided that the equivalent roughness height of the sediment bed is available. However, it should be noted that the present formula was calibrated using the data largely for naturally-worn coarse grains. Further studies should be conducted to investigate viscous effect on the average velocity of fine bedload grains.

Acknowledgements

This study was partially supported by the Open Fund of the State Key Laboratory of Hydraulics and Mountain River Engineering, Sichuan University, Chengdu, P. R. China.

Notation

The following symbols are used in this paper:

C_D drag coefficient;

c_1 coefficient;

c_2 coefficient;

c_3 coefficient;

D grain diameter;

D_* dimensionless grain diameter;

F_D drag force;

F_L lift force;

F_R bed resistance force;

g gravitational acceleration;

h flow depth;

k_s equivalent roughness height of the channel bed;

k_s^+ $= u_* k_s/\nu$;

m exponent;

Re_* $= u_* D/\nu$;

S channel slope;

s distance from the center of moving grain to boundary;

T temperature;

T_* transport stage parameter;

u_* shear velocity;

u_b unobstructed, near-bed flow velocity at y_b;

u_s average grain velocity;

W submerged grain weight;

y_b representative distance from the center of moving grain to channel bed;

y_b^+ $= u_* y_b/\nu$;

α friction angle;

β slope angle;

Δ effective specific density $[= (\rho_s - \rho)/\rho]$;

θ dimensionless bed shear stress or Shields number;

θ_c critical Shields number for incipient sediment motion;

ν kinematic viscosity of fluid;

ρ fluid density;

ρ_s grain density; and

χ dimensionless grain velocity.

References

Abbott, J. E., and Francis, J. R. D. (1977). "Saltation and suspension trajectories of solid grains in a water stream." Philosophical Transactions of the Royal Society a-Mathematical Physical and Engineering Sciences, 284(1321), 225-254.

Bagnold, R. A. (1973). "The nature of saltation and of `bed-load' transport in water." Proceedings of the Royal Society of London, Series A (Mathematical and Physical Sciences), 332(1591), 473-504.

Bathurst, J. C., Li, R. M., and Simons, D. B. (1981). "Resistance equation for large-scale roughness." Journal of the Hydraulics Division-ASCE, 107(12), 1593-1613.

Bounvilay, B. (2003). "Transport velocities of bedload particles in rough open channel flows." Ph.D Ph.D Colorado State University.

Bridge, J. S., and Dominic, D. F. (1984). "Bed-load grain velocities and sediment transport rates." Water Resources Research, 20(4), 476-490.

Buffington, J. M., Dietrich, W. E., and Kirchner, J. W. (1992). "Friction angle measurements on a naturally formed gravel streambed - implications for critical boundary shear-stress." Water Resources Research, 28(2), 411-425.

Cheng, N. S. (1997). "Simplified settling velocity formula for sediment particle." Journal of Hydraulic Engineering-ASCE, 123(2), 149-152.

Cheng, N. S. (2002). "Exponential formula for bedload transport." Journal of Hydraulic Engineering-ASCE, 128(10), 942-946.

Cheng, N. S. (2008). "Comparison of settling-velocity-based formulas for threshold of sediment motion." Journal of Hydraulic Engineering-ASCE, 134(8), 1136-1141.

Cheng, N. S. (2009). "Comparison of formulas for drag coefficient and settling velocity of spherical particles." Powder Technology, 189(3), 395-398.

Cheng, N. S., Nguyen, H. T., Zhao, K. F., and Tang, X. N. (2011). "Evaluation of Flow Resistance in Smooth Rectangular Open Channels with Modified Prandtl Friction Law." Journal of Hydraulic Engineering-ASCE, 137(4), 441-450.

Chien, N., and Wan, Z. (1999). Mechanics of sediment transport, American Society of Civil Engineers, Reston, Va.

Einstein, H. A. (1950). The bed-load function for sediment transportation in open channel flows, U.S. Dept. of Agriculture, Washington.

Ferguson, R. (2007). "Flow resistance equations for gravel- and boulder-bed streams." Water Resources Research, 43(5).

Fernandez Luque, R. (1974). "Erosion and transport of bed-load sediment."Ph.D., Delft University of Technology.

Fernandez Luque, R., and van Beek, R. (1976). "Erosion and transport of bed-load sediment." Journal of Hydraulic Research, 14(2), 127-144.

Francis, J. R. D. (1973). "Experiments on the motion of solitary grains along the bed of a water-stream." Proc. Roy. Soc. London, Series A(332 , no.1591), 1973.

Fredsoe, J., and Deigaard, R. (1992). Mechanics of coastal sediment transport, World Scientific, Singapore.

Hu, C. H., and Hui, Y. J. (1996). "Bed-load transport .1. Mechanical characteristics." Journal of Hydraulic Engineering-ASCE, 122(5), 245-254.

Johnston, C. E., Andrews, E. D., and Pitlick, J. (1998). "In situ determination of particle friction angles of fluvial gravels." Water Resources Research, 34(8), 2017-2030.

Julien, P. Y., and Bounvilay, B. (2013). "Velocity of rolling bed load particles." Journal of Hydraulic Engineering-ASCE, 139(2), 177-186.

Laursen, E. M. (1999). "Pickup probability for sediment entrainment - Discussion." Journal of Hydraulic Engineering-ASCE, 125(7), 786-787.

Lavelle, J. W., and Mofjeld, H. O. (1987). "Do critical stresses for incipient motion and erosion really exist." Journal of Hydraulic Engineering-ASCE, 113(3), 370-385.

Lee, H. Y., Chen, Y. H., You, J. Y., and Lin, Y. T. (2000). "Investigations of continuous bed load saltating process." Journal of Hydraulic Engineering-ASCE, 126(9), 691-700.

Lee, H. Y., and Hsu, I. S. (1994). "Investigation of saltating particle motions." Journal of Hydraulic Engineering-ASCE, 120(7), 831-845.

Miller, R., and Byrne, R. J. (1966). "The angle of repose for a single grain on a fixed rough bed." Sedimentology(6), 303-314.

Nakagawa, H., and Tsujimoto, T. (1981). "Hydrodynamic drag force acting upon a spherical particle on a rough bed composed of identical particles." Bulletin of the Disaster Prevention Research Institute, 31(2), 115-130.

Niño, Y., and García, M. (1998). "Experiments on saltation of sand in water." Journal of Hydraulic Engineering-ASCE, 124(10), 1014-1025.

Niño, Y., García, M., and Ayala, L. (1994). "Gravel saltation .1. Experiments." Water Resources Research, 30(6), 1907-1914.

Paintal, A. S. (1971). "A stochastic model of bed load transport." Journal of Hydraulic Research, 9(4), 527-554.

Parsons, D. A. (1972). "The speeds of sand grains in laminar flow over a smooth bed." Sedimentation: Symposium to Honor Professor H. A. Einstein, H. W. Shen, ed., Colorado State University, Fort Collins, Colorado.

Recking, A., Frey, P., Paquier, A., Belleudy, P., and Champagne, J. Y. (2008). "Bed-load transport flume experiments on steep slopes." Journal of Hydraulic Engineering-ASCE, 134(9), 1302-1310.

Schmeeckle, M. W., Nelson, J. M., and Shreve, R. L. (2007). "Forces on stationary particles in near-bed turbulent flows." Journal of Geophysical Research-Earth Surface, 112(F02003), 1-21.

van Rijn, L. C. (1982). "Equivalent roughness of alluvial bed." Journal of the Hydraulics Division-ASCE, 108(10), 1215-1218.

van Rijn, L. C. (1984). "Sediment transport .1. Bed-load transport." Journal of Hydraulic Engineering-ASCE, 110(10), 1431-1456.

Whitehouse, R. J. S., Soulsby, R. L., and Damgaard, J. S. (2000). "Inception of sediment transport on steep slopes - Discussion." Journal of Hydraulic Engineering-ASCE, 126(7), 553-555.

Wiberg, P. L., and Smith, J. D. (1987). "Calculations of the critical shear-stress for motion of uniform and heterogeneous sediments." Water Resources Research, 23(8), 1471-1480.

Wu, W. (2008). "Computational river dynamics." Taylor & Francis, London ; New York, xiii, 494 p.

Wu, W., Altinakar, M., and Wang, S. S. Y. (2006). "Depth average analysis of hysteresis between flow and sediment transport under unsteady conditions." International Journal of Sediment Research, 21(2), 101-112.

Table 1. Previous Formulas for Calculating Bedload Grain Velocity

Investigator	χ	Note
Einstein (1950)	$c\theta'^{0.5}$	c = constant; θ′ is grain-related Shields number
Bagnold (1973)	$U/(\Delta gD)^{0.5} - 5.75\theta^{0.5}\log[0.37h/(nD)] - w/(\Delta gD)^{0.5}$	$n = 1.4(\theta/\theta_c)^{0.6}$; h = flow depth; U = depth-averaged flow velocity; w = settling velocity
Fernandez Luque and van Beek (1976)	$11.5(\theta^{0.5} - 0.7\theta_c^{0.5})$	
Abbott and Francis (1977)	$c(\theta^{0.5} - 0.14)$	c = 13.5-14.3
van Rijn (1984)	$(9+2.6\log D_*)\theta^{0.5} - 8\theta_c^{0.5}$	
Bridge and Dominic (1984)	$c(\theta^{0.5} - \theta_c^{0.5})$	c = 6.6-15.6
Fredsoe and Deigaard (1992)	$10(\theta^{0.5} - 0.7\ \theta_c^{0.5})$	
Hu and Hui (1996)	$19.5\theta^{0.5} - 5.1\theta_c^{0.5}$ (for smooth bed) $11.9\theta^{0.5} - 5.2\theta_c^{0.5}$ (for rough bed)	
Lee and Hsu (1994)	$11.5\theta^{0.5}(\theta - \theta_c)^{0.174}$	
Lee et al. (2000)	$3.14D_*^{0.17}(\theta/\theta_c - 1)^{0.18}\theta^{0.5}$	
Wu (2008)	$1.64(\theta/\theta_c - 1)^{0.5}$	
Julien and Bounvilay (2013)	$11.5\theta^{0.95}D_*^{0.21}(D/k_s)^{0.36}\Delta^{-0.28}$	

Table 2. Summary of Experimental Data Used for Analysis

Investigator	Bed Roughness height k_s (mm)	Tested grain			Shields number θ	Dimensionless grain diameter D_*	No. of observations
		Shape	Diameter D (mm)	Specific gravity ρ_s/ρ			
(1) Smooth bed ($k_s << D$)							
Parsons (1972)		spherical	0.25-0.85		0.0037-0.041	7-26	31
Hu and Hui (1996)		spherical; angular	2.3-3.6	1.04-2.65	0.15-1.41	16.8-88.5	10
Julien and Bounvilay (2013)		spherical; angular	1.57-29.3	2.6-8.02	0.000076-0.016	62-778	172
Present study		spherical	11	1.14-2.59	0.0019-0.16	136-306	52
(2) Rigid sediment bed ($k_s \approx D$)							
Francis (1973)	7.5	naturally-worn	7.5	1.04-2.42	0.042-2.41	55-180	30
Abbott and Francis (1977)	7.2	naturally-worn	8.82	1.20-2.86	0.035-1.12	110-232	68
Lee and Hsu (1994)	1.36	naturally-worn	1.36	2.64	0.059-0.50	34-62	9
Nina and Garcia (1998)	0.5	naturally-worn	0.5	2.65	0.053-0.127	13	6
Lee et al. (2000)	6		6	1.08-1.38	0.066-0.55	55-93	6

Julien and Bounvilay (2013)	2.4-3.4	naturally worn	2.4-3.4	2.65	0.035-0.067	61-86	6
Present study	11	spherical	11	1.14-2.59	0.012-0.16	136-306	44
(3) Rigid sediment bed ($k_s < D$)							
Julien and Bounvilay (2013)	1.2-3.4	spherical; angular	2.4-29.3	2.6-8.02	0.00079-0.090	61-797	351
Lee and Hsu (1994)	1.36	Naturally-worn	2.47	2.64	0.142-0.199	62	3
(4) Mobile sediment bed ($k_s > D$)							
Fernadez Luque and van Beek (1974)		naturally-worn	0.9-3.3	1.34-4.58	0.044-0.076	22-83	17
Nino and Garcia (1994)		naturally-worn	15-31	2.65	0.084-0.15	379-784	6

Table3(R1)
Click here to download Table: Table3.doc

Table 3. Summary of Experimental Data Collected in the Present Study (sphere diameter = 11 mm, and channel width = 100 mm).

Test No.	Bed roughness height k_s(m)	Δ (= ρ_s/ρ - 1)	Flow depth h (m)	Slope	Shear velocity u_* (m/s)	Grain velocity u_s(m/s)
1	0.011	0.14	0.015	0.005	0.028	0.196
2	0.011	0.14	0.015	0.007	0.032	0.230
3	0.011	0.14	0.015	0.009	0.037	0.277
4	0.011	0.14	0.015	0.011	0.040	0.321
5	0.011	0.14	0.015	0.012	0.042	0.350
6	0.011	0.14	0.015	0.014	0.045	0.373
7	0.011	0.14	0.015	0.016	0.049	0.412
8	0.011	0.48	0.0165	0.008	0.037	0.181
9	0.011	0.48	0.018	0.008	0.038	0.191
10	0.011	0.48	0.0195	0.008	0.040	0.201
11	0.011	0.48	0.0215	0.008	0.042	0.215
12	0.011	0.48	0.014	0.015	0.045	0.272
13	0.011	0.48	0.015	0.015	0.047	0.293
14	0.011	0.48	0.016	0.015	0.048	0.303
15	0.011	0.48	0.0195	0.015	0.054	0.351
16	0.011	0.48	0.013	0.019	0.049	0.327
17	0.011	0.48	0.014	0.019	0.051	0.340
18	0.011	0.48	0.015	0.019	0.053	0.369
19	0.011	0.48	0.017	0.019	0.056	0.398
20	0.011	0.48	0.015	0.004	0.024	0.078
21	0.011	0.48	0.015	0.006	0.030	0.144
22	0.011	0.48	0.015	0.007	0.033	0.172
23	0.011	0.48	0.015	0.011	0.041	0.269
24	0.011	0.48	0.015	0.016	0.048	0.337
25	0.011	0.48	0.015	0.020	0.054	0.388
26	0.011	0.48	0.015	0.021	0.056	0.409
27	0.011	0.48	0.015	0.024	0.060	0.443
28	0.011	0.48	0.015	0.027	0.063	0.490
29	0.011	0.48	0.015	0.029	0.065	0.488
30	0.011	1.59	0.014	0.029	0.063	0.233
31	0.011	1.59	0.0145	0.031	0.066	0.302
32	0.011	1.59	0.014	0.031	0.065	0.281
33	0.011	1.59	0.0155	0.024	0.060	0.203
34	0.011	1.59	0.015	0.024	0.059	0.185
35	0.011	1.59	0.015	0.015	0.047	0.114
36	0.011	1.59	0.0165	0.015	0.049	0.137
37	0.011	1.59	0.015	0.019	0.053	0.202
38	0.011	1.59	0.0165	0.019	0.055	0.215

39	0.011	1.59	0.015	0.022	0.057	0.241
40	0.011	1.59	0.0165	0.022	0.060	0.279
41	0.011	1.59	0.015	0.025	0.061	0.306
42	0.011	1.59	0.0165	0.025	0.064	0.318
43	0.011	1.59	0.015	0.028	0.064	0.346
44	0.011	1.59	0.0165	0.028	0.067	0.389
45	0	1.59	0.013	0.003	0.0181	0.229
46	0	1.59	0.016	0.003	0.0201	0.251
47	0	1.59	0.019	0.003	0.0219	0.265
48	0	1.59	0.022	0.003	0.0236	0.290
49	0	1.59	0.013	0.005	0.0258	0.361
50	0	1.59	0.0155	0.005	0.0282	0.387
51	0	1.59	0.018	0.005	0.0304	0.415
52	0	1.59	0.013	0.010	0.0354	0.448
53	0	1.59	0.0165	0.010	0.0399	0.481
54	0	1.59	0.018	0.010	0.0417	0.502
55	0	1.59	0.0125	0.013	0.0400	0.521
56	0	1.59	0.014	0.013	0.0423	0.531
57	0	1.59	0.016	0.013	0.0452	0.558
58	0	1.59	0.0175	0.013	0.0473	0.568
59	0	1.59	0.013	0.015	0.0441	0.591
60	0	1.59	0.014	0.015	0.0457	0.614
61	0	1.59	0.016	0.015	0.0489	0.633
62	0	1.59	0.0165	0.015	0.0497	0.639
63	0	0.48	0.013	0.003	0.0181	0.242
64	0	0.48	0.016	0.003	0.0201	0.271
65	0	0.48	0.019	0.003	0.0219	0.289
66	0	0.48	0.022	0.003	0.0236	0.308
67	0	0.48	0.013	0.005	0.0258	0.373
68	0	0.48	0.0155	0.005	0.0282	0.408
69	0	0.48	0.018	0.005	0.0304	0.453
70	0	0.48	0.013	0.010	0.0354	0.457
71	0	0.48	0.0165	0.010	0.0399	0.513
72	0	0.48	0.018	0.010	0.0417	0.547
73	0	0.48	0.0125	0.013	0.0400	0.533
74	0	0.48	0.014	0.013	0.0423	0.547
75	0	0.48	0.016	0.013	0.0452	0.592
76	0	0.48	0.0175	0.013	0.0473	0.613
77	0	0.48	0.0165	0.015	0.0497	0.684
78	0	0.48	0.0155	0.015	0.0481	0.673
79	0	0.48	0.014	0.015	0.0457	0.668
80	0	0.14	0.013	0.003	0.0181	0.268
81	0	0.14	0.016	0.003	0.0201	0.304
82	0	0.14	0.019	0.003	0.0219	0.328

83	0	0.14	0.022	0.003	0.0236	0.351
84	0	0.14	0.013	0.005	0.0258	0.391
85	0	0.14	0.0155	0.005	0.0282	0.441
86	0	0.14	0.018	0.005	0.030	0.496
87	0	0.14	0.013	0.010	0.035	0.495
88	0	0.14	0.0165	0.010	0.040	0.556
89	0	0.14	0.018	0.010	0.042	0.596
90	0	0.14	0.0125	0.013	0.040	0.577
91	0	0.14	0.014	0.013	0.042	0.599
92	0	0.14	0.016	0.013	0.045	0.640
93	0	0.14	0.0175	0.013	0.047	0.666
94	0	0.14	0.0165	0.015	0.050	0.747
95	0	0.14	0.0155	0.015	0.048	0.738
96	0	0.14	0.014	0.015	0.046	0.711

Table 4. Summary of Prediction Errors

Investigator	Average error (%)
Rough beds with $k_s = D$	
Fernandez Luque and van Beek (1976)	23.1
van Rijn (1984)	14.2
Fredsoe and Deigaard (1992)	32.0
Lee and Hsu (1994)	16.2
Hu and Hui (1996)	11.0
Lee et al. (2000)	13.9
Wu (2008)	37.1
Julien and Bounvilay (2013)	145.3
Present study	9.9
Rough beds with $k_s \leq D$	
Julien and Bounvilay (2013)	45.7
Present study	15.7
Smooth and rough beds	
Present study	18.2

Figure1(R1)
Click here to download Figure: Figure 1.pdf

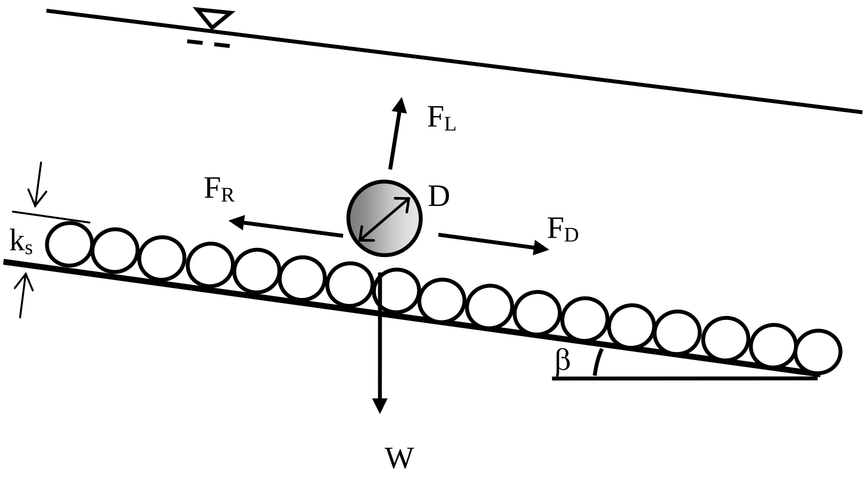

Figure 1. Forces exerting on a solitary bedload grain.

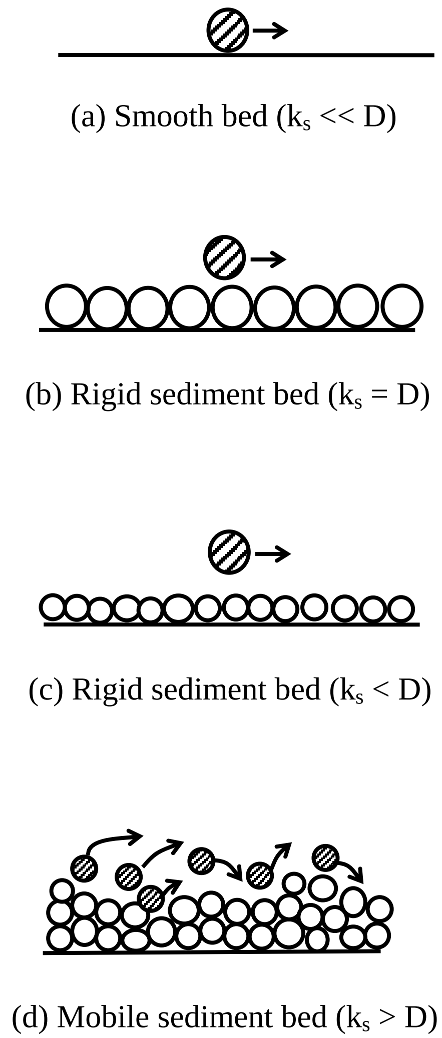

Figure 2. Bedload grains moving over four different channel beds.

Figure3
Click here to download Figure: Figure 3.pdf

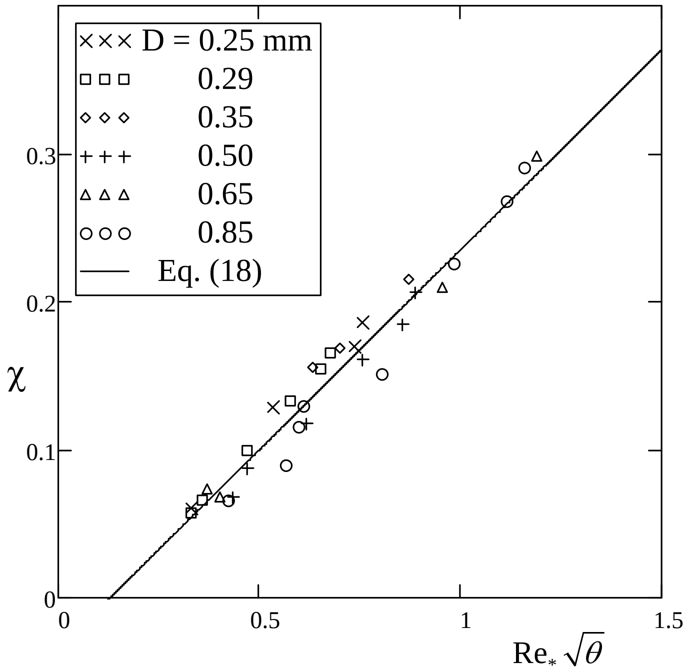

Figure 3. Variation of dimensionless bedload grain velocity for laminar flows over a smooth bed. The experiments were conducted with glass beads (*Parsons* 1972). Eq. (18) was plotted by taking c_3 = 0.27 and the last term as a constant (= 0.03).

Figure4

Click here to download Figure: Figure 4.pdf

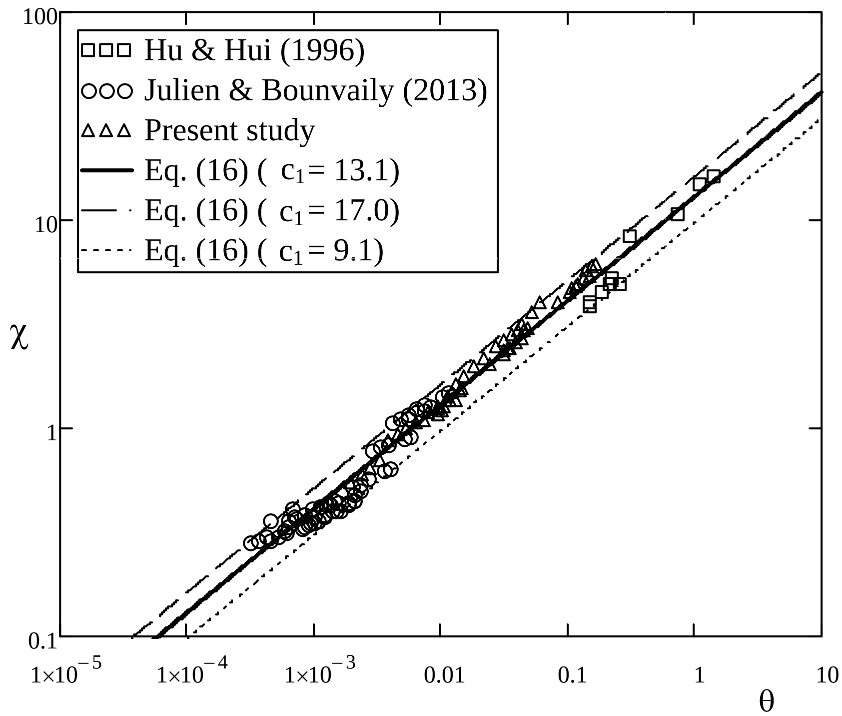

Figure 4. Variation of dimensionless grain velocity for turbulent flows over a smooth bed. Eq. (16) was used to fit the data with c_1 = 13.1 (with a variation of ±30%) and c_2 = 0.

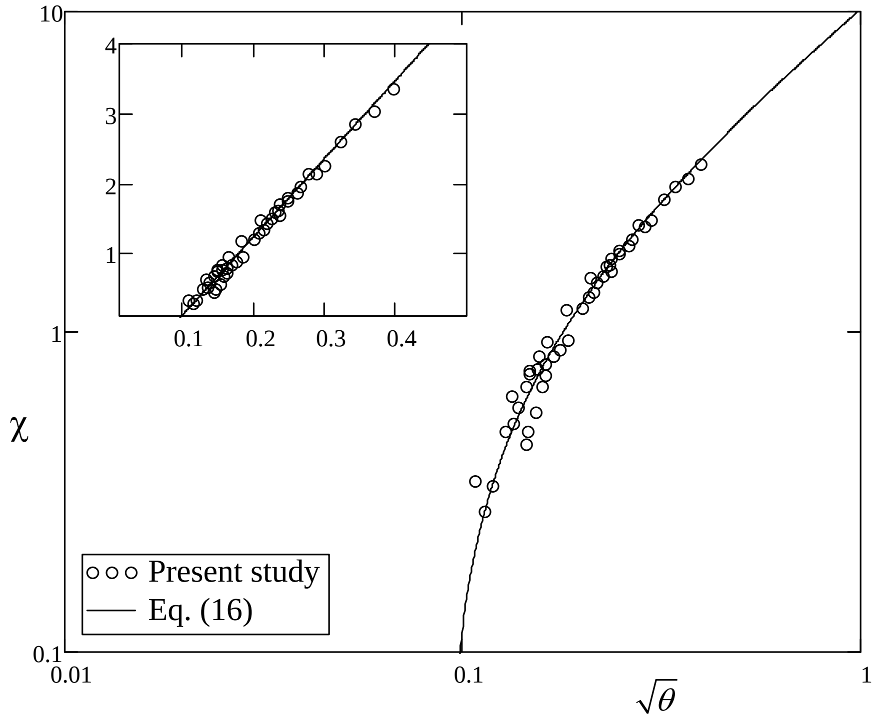

Figure 5. Variation of dimensionless grain velocity for spheres with $k_s = D$. The data were collected in the present study and fitted with Eq. (16) by taking $c_1 = 12.1$ and $c_2 = 1.0$. The insert shows the same data plotted with linear coordinates.

Figure6

Click here to download Figure: Figure 6.pdf

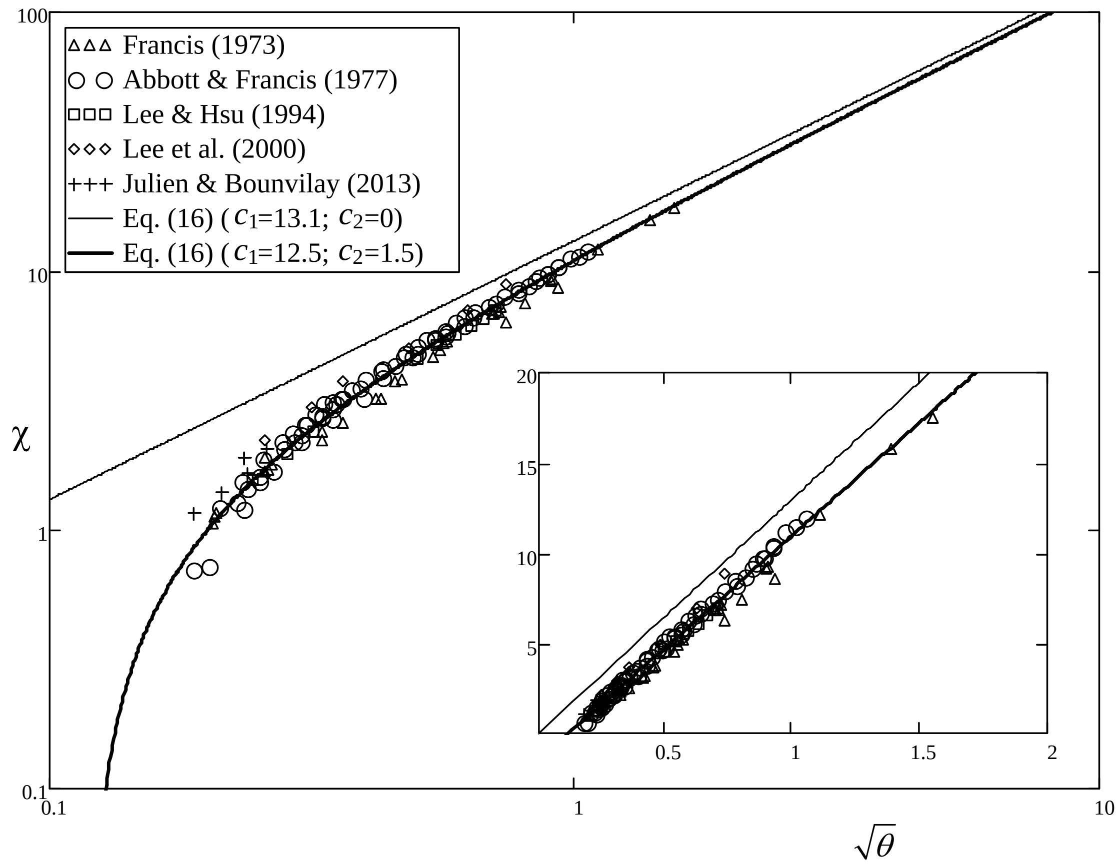

Figure 6. Variation of dimensionless grain velocity for rough beds comprising naturally-worn grains with $k_s = D$. Eq. (16) was fitted to the data by taking $c_1 = 12.5$ and $c_2 = 1.5$. The insert shows the same data plotted with linear coordinates.

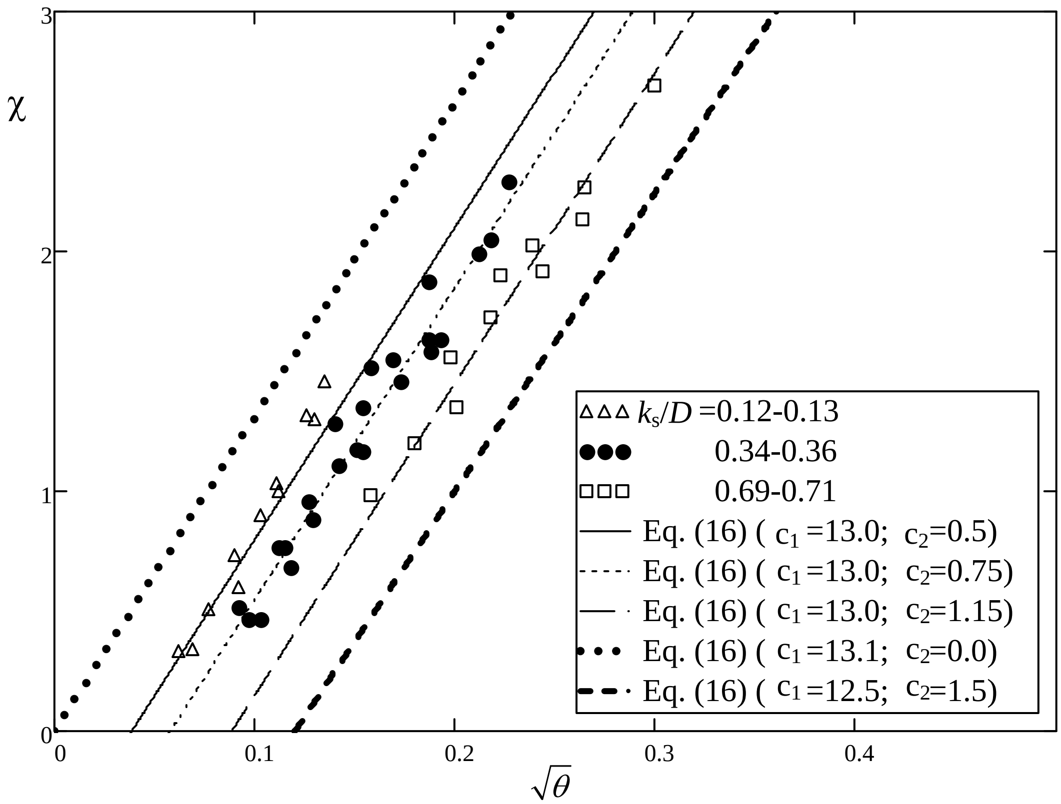

Figure 7. Effects of k_s/D on the relationship of χ-$\sqrt{\theta}$. The data were reported by Julien and Bounvilay (2013). Eq. (16) was superimposed with different coefficients. The uppermost line represents the data for the smooth bed while the lowest line represents the data for $k_s = D$.

Figure8

Click here to download Figure: Figure 8.pdf

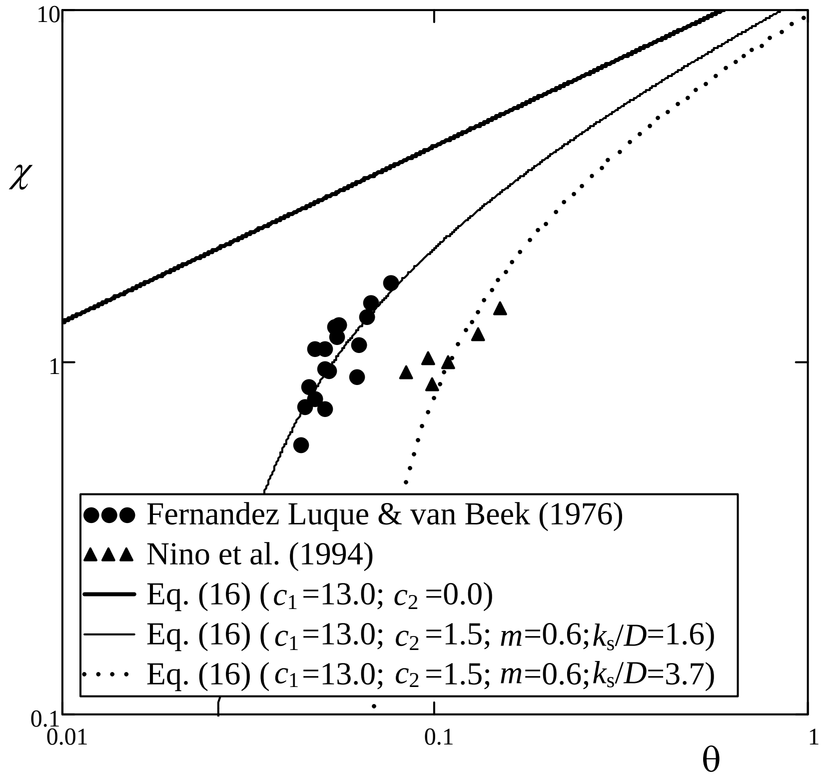

Figure 8. Fitting of Eq. (16) to experimental data for the mobile bed conditions.

Figure9(R2)
Click here to download Figure: Figure 9 (R2).pdf

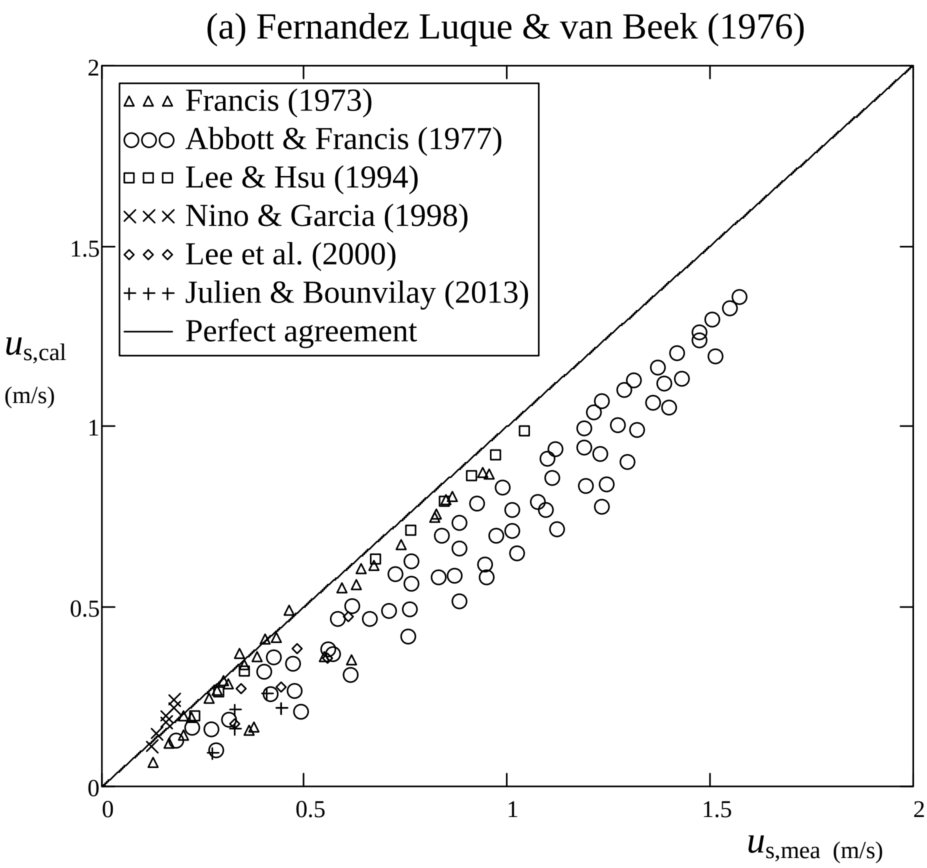

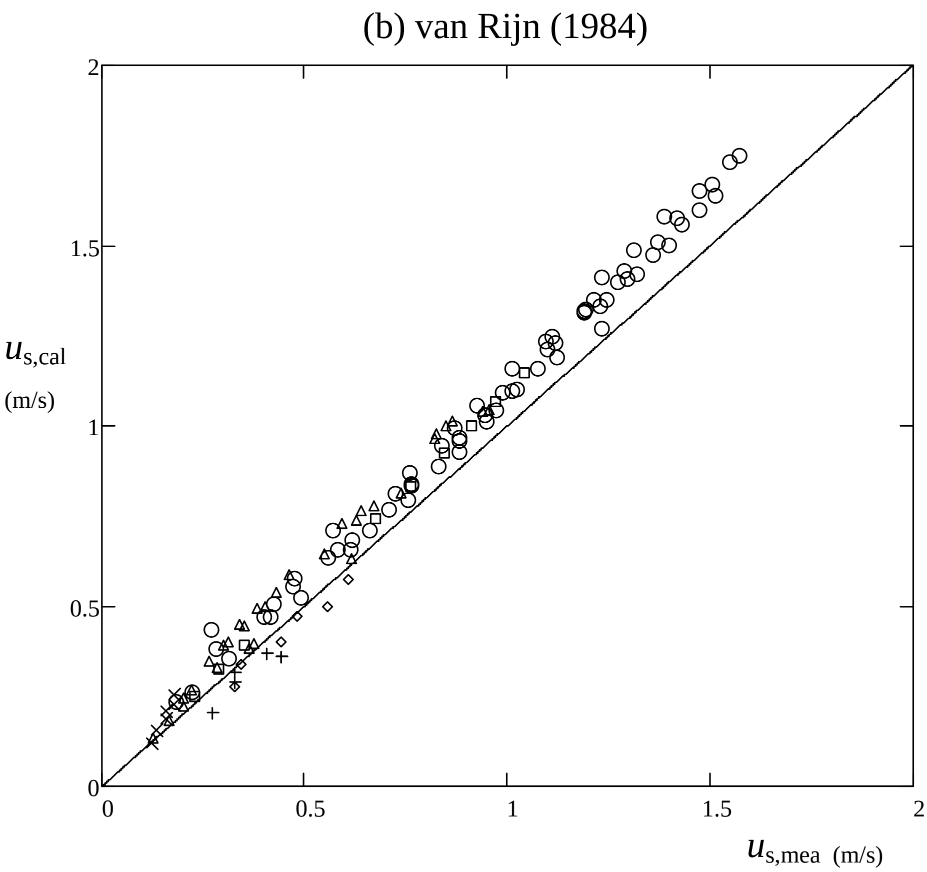

(c) Fredsoe & Deigaard (1992)

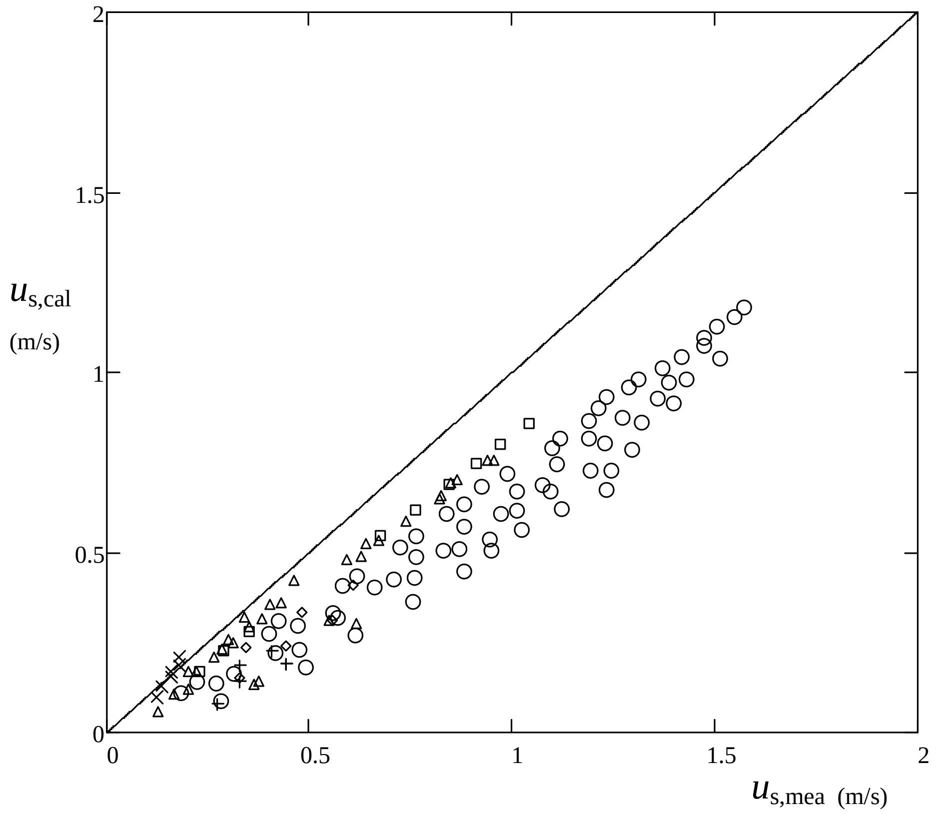

(d) Lee & Hsu (1994)

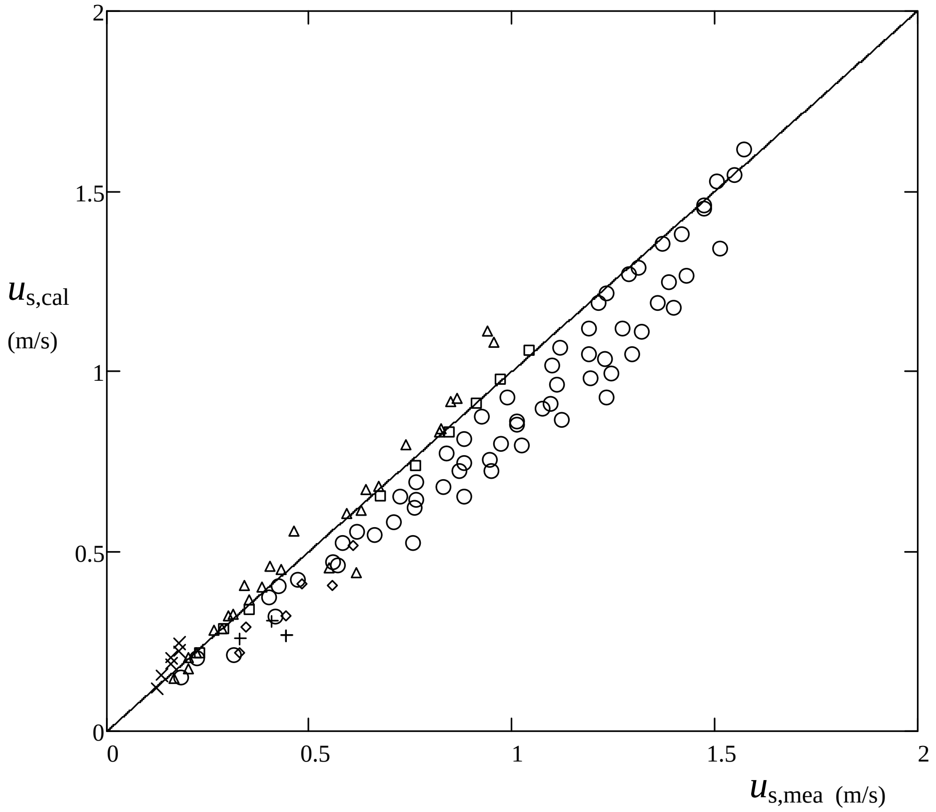

(e) Hu & Hui (1996)

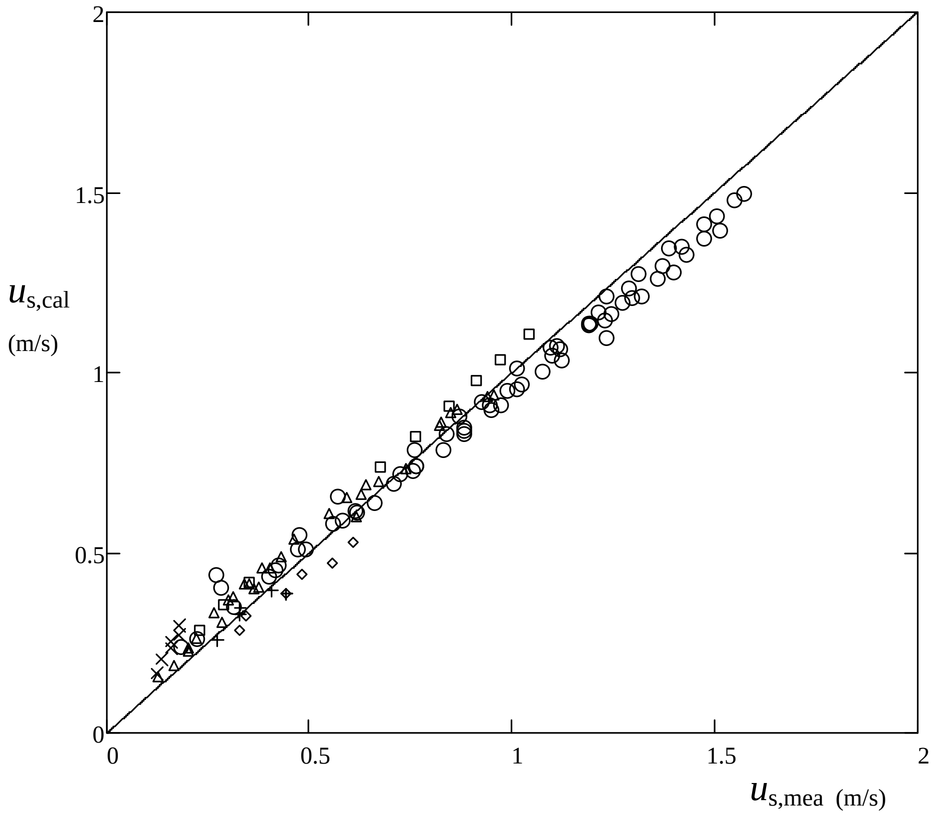

(f) Lee et al. (2000)

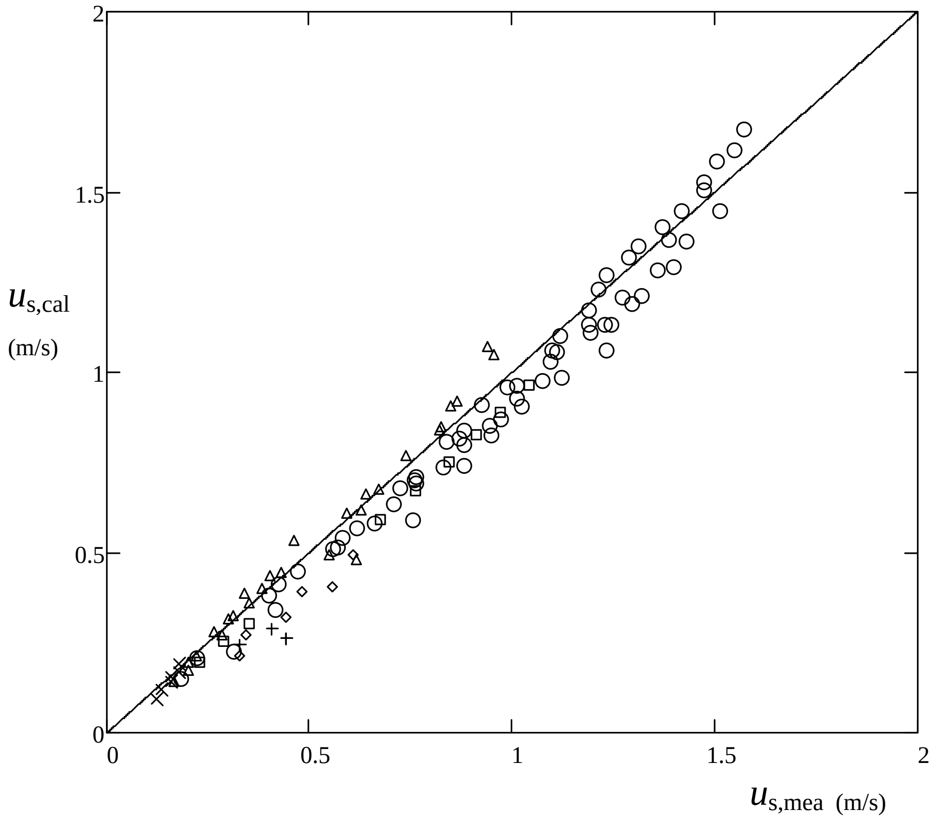

(g) Wu (2008)

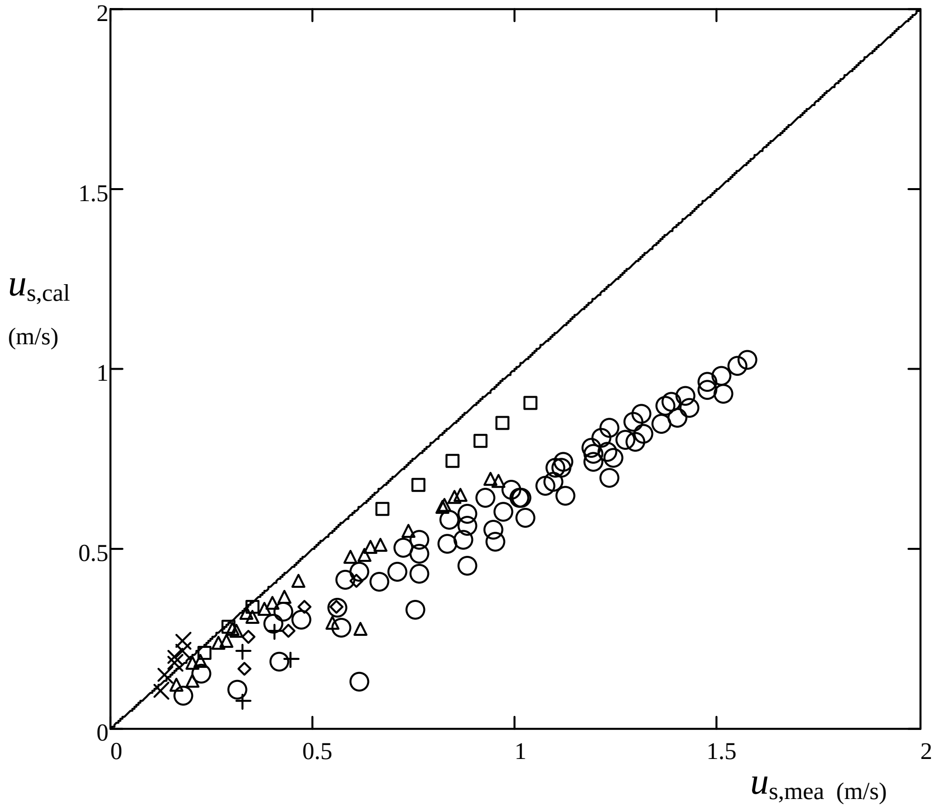

(h) Julien & Boundilay (2013)

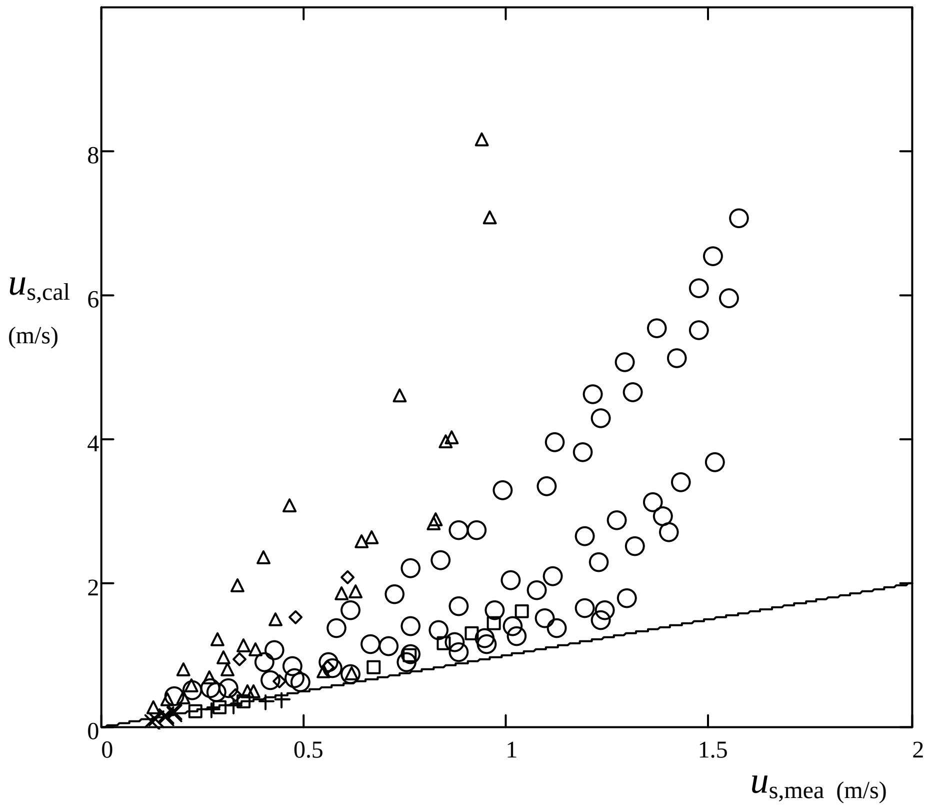

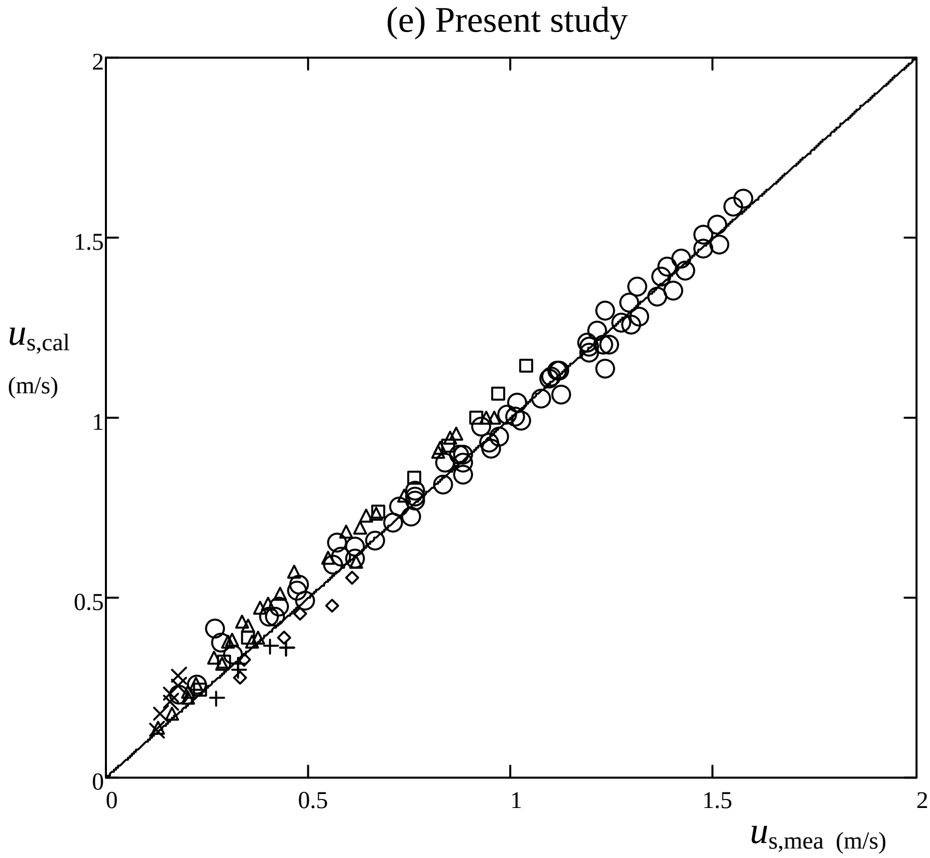

Figure 9. Comparison of calculated and measured bedload grain velocities for rough beds comprising naturally-worn grains with $k_s = D$. The same symbols are used for figures (a) to (h).

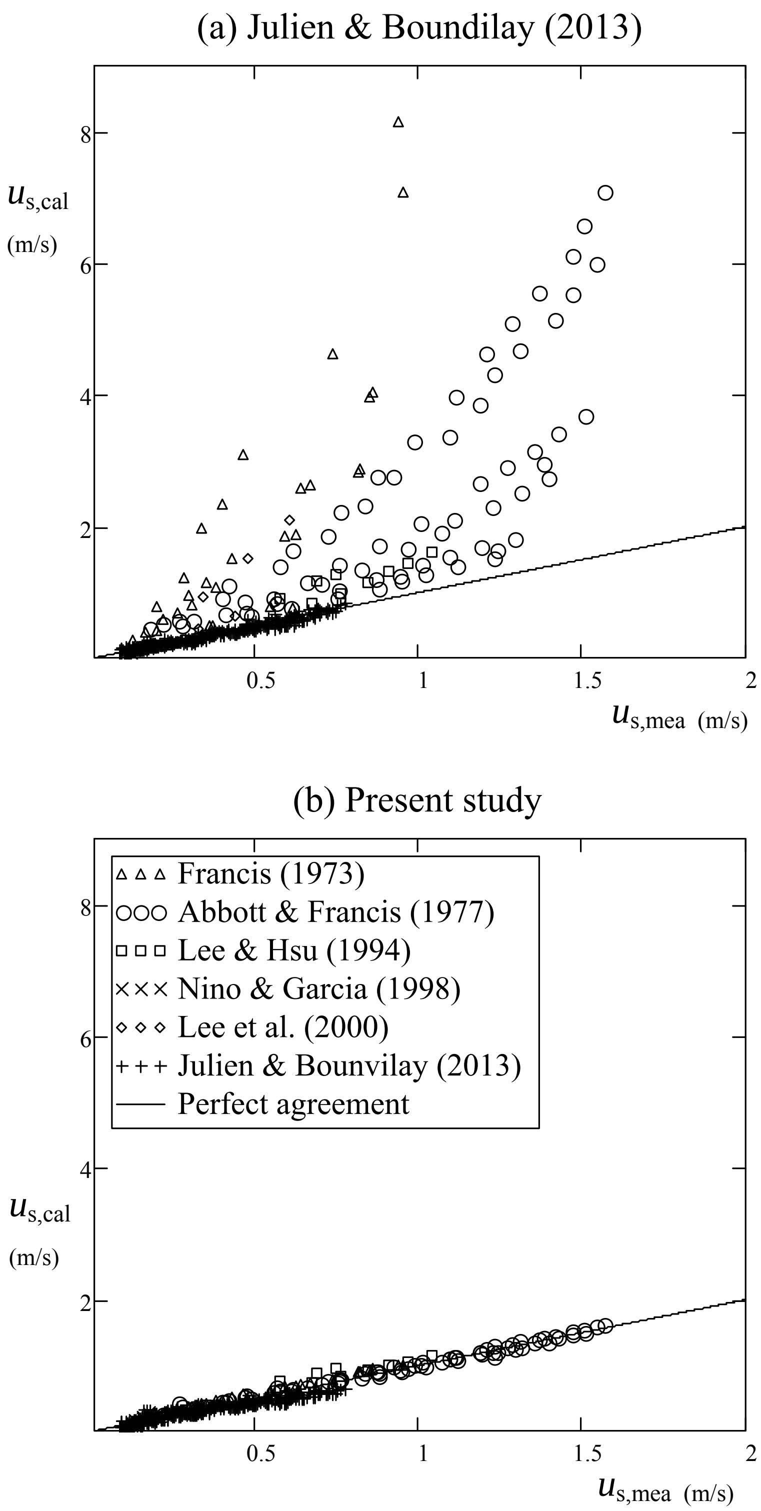

Figure 10. Comparison of calculated and measured bedload grain velocities for rough beds comprising naturally-worn grains with $k_s \leq D$. The same symbols are used for figures (a) and (b).

Figure11

Click here to download Figure: Figure 11.pdf

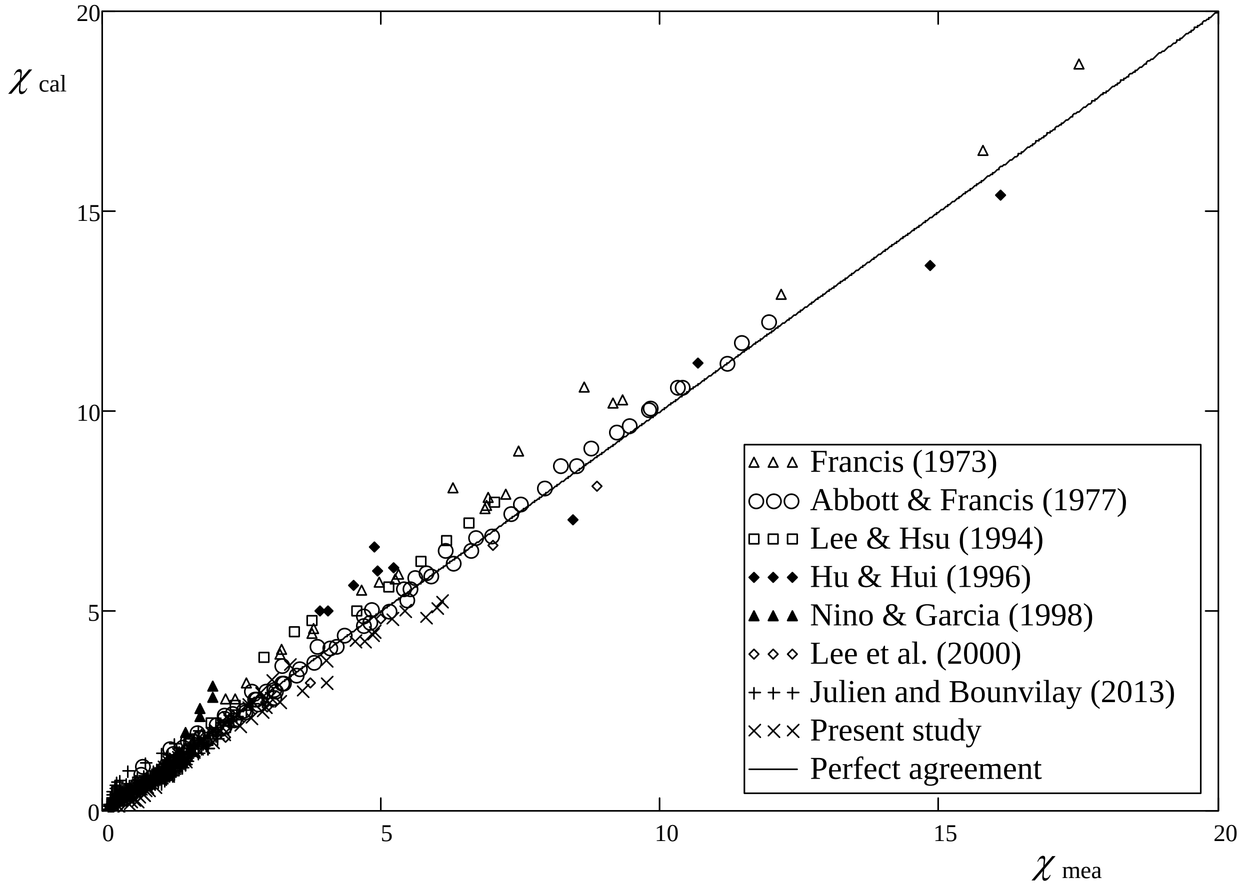

Figure 11. Comparison of calculated and measured dimensionless bedload grain velocities for both smooth and rough bed conditions. No differentiation was made between spherical and non-spherical grains. Eq. (16) with c_1 = 13, c_2 = 1.5 and m = 0.6 was used for calculations.

Figure Captions

Fig. 1. Forces exerting on a solitary bedload grain.

Fig. 2. Bedload grains moving over four different channel beds.

Fig. 3. Variation of dimensionless bedload grain velocity for laminar flows over a smooth bed. The experiments were conducted with glass beads (Parsons 1972). Eq. (18) was plotted by taking $c_3 = 0.27$ and the last term as a constant (= 0.03).

Fig. 4. Variation of dimensionless grain velocity for turbulent flows over a smooth bed. Eq. (16) was used to fit the data with $c_1 = 13.1$ (with a variation of ±30%) and $c_2 = 0$.

Fig. 5. Variation of dimensionless grain velocity for spheres with $k_s = D$. The data were collected in the present study and fitted with Eq. (16) by taking $c_1 = 11.2$ and $c_2 = 1.0$. The insert shows the same data plotted with linear coordinates.

Fig. 6. Variation of dimensionless grain velocity for rough beds comprising naturally-worn grains with $k_s \approx D$. Eq. (16) was used to fit the data with $c_1 = 12.5$ and $c_2 = 1.5$. The insert shows the same data plotted with linear coordinates.

Fig. 7. Effects of k_s/D on the relationship of χ- $\sqrt{\theta}$. The data were reported by Julien and Bounvilay (2013). Eq. (16) was superimposed with different coefficients. The uppermost line represents the data for the smooth bed while the lowest line represents the data for $k_s \approx D$.

Fig. 8. Fitting of Eq. (16) to experimental data for the mobile bed conditions.

Fig. 9. Comparison of calculated and measured bedload grain velocities for rough beds comprising naturally-worn grains with $k_s \approx D$. The same symbols are used in figures (a) to (e).

Fig. 10. Comparison of calculated and measured bedload grain velocities for rough beds comprising naturally-worn grains with $k_s \leq D$. The same symbols are used in figures (a) and (b).

Fig. 11. Comparison of calculated and measured dimensionless bedload grain velocities for both smooth and rough bed conditions. No differentiation was made between spherical and non-spherical grains. Eq. (16) with $c_1 = 13$, $c_2 = 1.5$ and $m = 0.6$ was used for calculations.